The 47th Annual Scientific Meeting of Himpunan Ahli Geofisika Indonesia
Malang, 10 – 13th of October 2022

Unlocking Shallow Play Potential by Implementing Frequency-dependent AVO attribute, East Java Basin

Haryono Haryanto*
Anwar Sadat*
Hotma Yusuf*

Abstract

The current improvements in the application of spectral decomposition have been intensively focused on direct hydrocarbon detection rather than structural interpretation. Current studies about hydrocarbon related frequency effects are predicted to be detectable on stacked seismic data. Furthermore, it has been suggested that low frequencies tend to show the highest sensitivity to fluid changes. Several studies have also shown evidence that hydrocarbon reservoirs have an amplitude-versus-offset (AVO) frequency dependence. There could be a correlation in frequency and variation amplitude with offset. Hydrocarbon bearing reservoir is indicated by frequency attribute which show the dispersion and attenuation related hydrocarbon presence and AVO which show the greatest changing amplitude with offset variation.

This paper intended to understand frequency anomaly in offset variation and to measure potential links between frequency and AVO effect related to hydrocarbon bearing gas sand reservoir and the application in revealing overlooking shallow hydrocarbon play potential. The Authors performed AVO effect prediction in several frequencies, then get the sensitivity of frequency and amplitude changing with offset variation related hydrocarbon presence in gas sandstone reservoir. The final product described gas sandstone reservoir in shallower play potential. Our trial on 3D seismic new reprocessed year of 2018 in East Java Basin shows the sensitivity of frequency dependent AVO in gas sand reservoir enable us to identify the interesting new hydrocarbon reservoir response.

Keyword: Frequency dependent AVO, attenuation factor, hydrocarbon reservoir, new shallow play potential.

Introduction

One of the most common and established techniques to identify hydrocarbon presence is by analyzing the amplitude variation with offset (AVO) utilizing the pre-stack seismic data (Mandong, 2021). AVO anomaly is a common way to investigate hydrocarbon bearing reservoir presence. Cross-ploting AVO makes the interpreter more confident in defining the good reservoir bearing hydrocarbon. The application of Spectral Decomposition has become the focus for geophysicists to provide an alternative set of hydrocarbon indicators based on time-frequency response (Haryono, 2017). Spectral decomposition produces a continuous time. Frequency analysis of the seismic trace, thus a single seismic trace can produce various time-frequencies ranging from low to high frequency. The character of seismic reflections from hydrocarbon-saturated zones have been widely believed to have a tendency of being low frequency and concentrated at or beneath the reservoir level; such effects are well known as low frequency shadow zone anomaly. This anomaly is probably caused by attenuation of high-frequency energy in the reservoir itself (Dilary and Eastwood, 1995; Mitchell et al., 1997), such that the local dominant frequency moves toward the low-frequency range. In fact, low frequency of spectral decomposition does not mean only hydrocarbon presence, it also correlates with lithology. It must be supported by attenuation analysis by comparing low and high frequency. In qualitative manner, it also creates the ambiguity spectral decomposition application. It has been suggested that the latest techniques of spectral decomposition can be used to identify hydrocarbon zones with anomalous frequency responses, which are represented by the attenuation factor (Castagna et al., 2003). The measurement of Q factor, which refers to the inverse of attenuation, is the important quantity in correlating the seismic property to saturated hydrocarbons (Haris and Haryono, 2012).

In this work, spectral Decomposition and AVO techniques performed into a cohesive workflow to generate reconnaissance attributes aimed at frequency anomaly detection related hydrocarbon presence in existing production reservoir interval and unlocking the new shallow play potential.

*Saka Muriah Energi Limited

Regional Geology

The Muriah region covers the Muriah Trough and West-15 Basin within the western edge of East Java Basin is the most structurally and stratigraphically complex of the Indonesian back-arc basin. Paleogene extensional tectonic and Neogene compressional tectonic controlled the deposition of sediment filling East Java Basin. Initial depositional in the Muriah area occurred prior to the Late Eocene and resulted in the accumulation of mainly continental and deltaic coarse-grained sands, conglomerates, and coals of Ngimbang unit in NE-SW trending half-grabens. This depositional phase terminated because of a tectonic phase of and/or eustatic sea level fall.

During the Late Eocene, a rise in sea level flooding large parts of the area and deposition of the limestones and shales of the Ngimbang Formation occurred. A sea level fall and subsequent erosion are thought to have removed parts of these deposits, particularly in the Muriah area. A transgression at the start of the Oligocene flooded most of the area and widespread carbonate deposition took place. Limited evidence suggests that marginal marine to supratidal deposits accumulated in the Muriah area during this time. A compressional phase and the 30Ma major eustatic sea level fall terminated this sequence. Subsequent erosion is thought to have removed most of these deposits in the Muriah area. Deposition restarted during the Late Oligocene when, initially, mainly continental, and deltaic deposits of the Kujung III Formation accumulated in the Muriah area. This late Oligocene reflects a transgression is considered the result of extensional tectonism in combination with the eustatic sea level rise starting at 26Ma. This gradual increase in depositional depth culminated in the widespread deposition of shallow marine deposits i.e., Kujung Formation in the Muriah area during the Early Miocene.

A short-lived regression stopped deposition in the Muriah area in the Early Miocene. Deposition restarted later in the Early Miocene as the result of the transgressive trend starting from 21 Ma. Widespread limestone sedimentation occurred over platform areas with local builds-up, continued sea level rise flooding most carbonate production and marine shales of the Tuban Formation were subsequently deposited. Deposition of this phase was followed by uplift, locally resulting in erosion during the initial stages of the Middle Miocene. This uplift resulted effectively in inversion over areas with well-developed Paleogene deposits.

Subsequent deposition in the Middle Miocene was strongly influenced by the overall eustatic sea level fall and increased clastic input as the result of uplift. Tawun formation, mainly shales overlain by sands, reflect a gradually shallowing depositional setting culminating in prograding delta shoreface. This phase is mainly recognized from the Muriah area. The major sea level fall at 10.5 Ma ends this phase and locally results in erosion of these deposits, possibly enhanced by continued tectonism throughout the Middle Miocene. Deposition restarted in the Late Miocene when a gradual transgressive trend flooded the Muriah area. Sedimentation culminated with the mainly shale and subordinate limestones of the Wonocolo formation. This transgressive trend continued in the Early Pliocene with the deposition of the shallow marine Ledok formation.

A compressional phase ends this stage of deposition, however subsequent transgression allowed the accumulation of the shallow marine limestones of the Paciran Formation during the Early to Late Pliocene.

Data And Methodology

Data Availability

The area of study is covered by 3D seismic survey vintage year of 2001. The data was acquired by using six Streamer with length 2400 meter and source depth 4 meters, through 196 channel system. The data was recorded for three seconds with final group interval of 12.5 meters and inline spacing 25 meters.

The data was reprocessed in 2018. The reprocessing seismic is designed to fix the noise to signal ratio and compartmentalization of reservoir. It utilized the latest technology of seismic Reprocessing such as FWI Q APSDM (Full Waveform Inversion and Q attenuation, depth migration). By combining those methods (Full waveform inversion to solve velocity issue depth migration for locating structure and fault in reliable depth position), it expected to get better understanding of reservoir characterization. The data used for this study : 1 well gas sand discovery and 3D seismic (figure 1)

Spectral Decomposition Continuous Wavelet Transform

Continuous Wavelet Transform (CWT) is a spectral decomposition algorithm for computing a time-frequency map for non-stationary signals. The CWT good performance compared to conventional method of producing a time-frequency map such as the Short Time Fourier Transform (STFT). STFT limits the time-frequency resolution by a pre-defined window length. In contrast, the CWT method does not require pre-selecting a window length and does not have a fixed time-frequency resolution over the time-frequency space. The CWT method uses dilatation and translation to produce time-scale (scalogram). CWT is defined by the formula:

$$F_w(\sigma,\tau) = < f(t),\psi(t) > = \int_{-\infty}^{\infty} f(t)\frac{1}{\sqrt{\sigma}}\psi^*\left(\frac{t-\tau}{\sigma}\right)dt \qquad (1)$$

Where ψ^* is the complex conjugate of $\psi(\sigma,\tau)$. F_w is the time-scale map (i.e. the scalogram). σ is scale parameter.

τ is translation parameter (Sinha, 2005). Translation parameter considers window location, with shifted window throughout signal. This parameter is associated with time information in transformation domain. High scale has a general view with no detail and low scale has detail view. CWT relation vs scale parameter with frequency is stated as follows:

$$Fa = Fc\frac{1}{\sigma\,\Delta} \qquad (2)$$

Where Fa is pseudo frequency associated with scale (Hz). Fc is the center frequency in wavelet (Hz). σ represents the scale and Δ is sampling time. In its implementation, the CWT is dependent on the selected wavelet. Our experiment shows that the complex Gaussian wavelet of fifth order provides proper time frequency results.

Amplitude Variation With Offset (Avo)

The two-term AVO approximation of Smith and Gidlow (1987) can be written as

$$R(\theta) \approx A(\theta)\frac{\Delta V_p}{V_p} + B(\theta)\frac{\Delta V_s}{V_s}, \qquad (3)$$

Where θ is the angle of incidence, and $A(\theta)$ and $B(\theta)$ can be derived in terms of the known velocity model. Common practice to simulate the AVO anomaly respons from seismic data is using the envelope AVO formula as stated:

$$(\text{Far} - \text{Near}) \times \text{Far} \qquad (7)$$

Following the theory of Wilson et al. (2009), in the frequency-dependent attribute scheme the reflection coefficient $R(\theta)$ and the (fractional) contrasts in P-wave and S-wave impedances, $\Delta V_p / V_p$ and $\Delta V_s / V_s$, are considered to vary with frequency due to dispersion in the material. Then Equation 2 can be written as:

$$R(\theta,f) \approx A(\theta)\frac{\Delta V_p}{V_p}(f) + B(\theta)\frac{\Delta V_s}{V_s}(f). \qquad (4)$$

Expanding Equation 3 as a first-order Taylor series around a reference frequency f_0,

$$R(\theta,f) \approx A(\theta)\frac{\Delta V_p}{V_p}(f_0) + (f-f_0)A(\theta)I_a + B(\theta)\frac{\Delta V_s}{V_s}(f_0) + (f-f_0)B(\theta)I_b, \qquad (5)$$

Where I_a and I_b are the derivatives of the velocity contrasts with respect to frequency evaluated at f_0:

$$I_a = \frac{d}{df}\left(\frac{\Delta V_p}{V_p}\right) \text{ and } I_b = \frac{d}{df}\left(\frac{\Delta V_s}{V_s}\right) \qquad (6)$$

Deriving ΔVp/ Vp and ΔVs/ Vs Δ at the reference frequency f0 by replacing R(θ f) with an appropriately balanced spectral amplitude at f0. Ia and Ib can be derived from Equation 4 by using least-squares method for the spectral amplitudes at a series of frequencies. When R(θ, f) is replaced by the spectral amplitude at different frequencies, Ia and Ib describe the derivative of the seismic velocity contrasts with frequency, related to P-wave dispersion and S-wave dispersion. Since the spectral amplitude is positive, we cannot handle phase reversals, and only the absolute values of Ia and Ib are meaningful. Considering that shear modulus is usually independent of the saturating fluid, the study focused on the Ia attribute to estimate the magnitude of P-wave dispersion, which is our new Frequency AVO attribute (Wu, et. al., 2012).

Result And Discussion

Study area has been conducted in East Java basin, currently production gas from LTA (Lower Tawun) interval. New FWI seismic reprocessing has been performed in 2018 and indicates good result for quantitative interpretation purposes.

Shallow potential has been introduced based on current maturation prospects. The shallow reservoir is identified as glauconitic feldsphatic sandstone which the member of Upper Wonocolo Formation to Ledok Formation. Sandstone has 10-20 feet of thickness with fine to coarse grained in size (figure 2). Though, the seismic is still showing amplitude anomaly (Figure 3). Indication of the shallow potential is also supported from total gas indication in HH-1 and HH-3 well. The total gas measured during drilling reached up to 200 units with C1 composition (figure 4).

The AVO has been used in predicting hydrocarbon presence by AVO anomaly, it is quite sensitive related gas sand interval reservoir. Current application of AVO performed in gather data and as function of offset, however, seismic data contained amplitude and frequency. In addition, frequency application has also been developed significantly. There could be relationship between AVO in frequency dependent. The application of spectral decomposition has been used in predicting hydrocarbon presence and become the focus of attention for geophysicists to provide an alternative set of hydrocarbon indicators based on the time-frequency response. The spectral decomposition CWT can be used properly in identifying the reservoir in shallower part with several frequency 15, 35 and 55 Hz, then described in AVO cross plot. Spectral Decomposition and AVO techniques are combined into a cohesive workflow to generate reconnaissance attributes aimed at frequency anomaly detection related hydrocarbon presence (figure 5).

Forward modeling AVO based on HH-1 and fluid replacement modeling indicates good evidence in the shallower part and has good similarity character with existing production interval in deeper part (figure 6). AVO from gather seismic also indicates good consistency with forward modeling and categorized as class 3 AVO (figure 7).

Low frequency from Spectral decomposition CWT indicated the possibility of hydrocarbon presence in shallower parts. Ambiguity arose when the magnitude of low frequency section has approximately the same bright anomaly between gas and water reservoirs. Overcoming this indeterminacy required deeper analysis of the data by integrating AVO analysis in frequency domain. The result of frequency dependent (15HZ, 35Hz and 55Hz) AVO indicated shallower interval reservoir has located in gas bearing reservoir in AVO crossplot. There is unique separation between frequency dependent AVO crossplot and conventional AVO crosplot, frequency dependent AVO shifted to the class 4 in AVO crossplot. However, it could be unique AVO crossplot curve for the frequency dependent AVO (figure 8 & 9).

Differentiation position in AVO classification between 15Hz, 35Hz and 55Hz could be affected by attenuation effect which shifts the value avoid water trend and supported by the envelope AVO. (figure 10). Integration frequency dependent AVO designated the AVO anomaly and attenuation, it describes lateral distribution of Hydrocarbon interval reservoir (figure 11). The integration between AVO and frequency dependent AVO can help the interpreter to predict hydrocarbon presence.

Conclusions

AVO and Frequency dependent AVO are good tools for predicting lateral distribution of gas sand and it also can unlock the shallow play potential,

Acknowledgement

The authors wish to express their appreciation to the Management and Director of Saka Energi Muriah Limited (SEML) who contributed in finalizing this paper, And also thanks to the members of Exploration Department who contributed on finalizing the internal permit for this paper.

References

Bransden, P.J.E., Mathews, S.J., 1992, Structural and Stratigraphic Evolution of the East Java Basin, Indonesia: Proceeding IPA 21st Annual Convention, p. 417-453

Carter, D. C., et. al., 2005. Interpretation Methods In The Exploration Of Oligocene-Miocene Carbonate Reservoirs, Offshore Northwest Madura, Indonesia: Indonesian Petroleum Association, Proceedings 30th Annual Convention, Jakarta.

Castagna, J, S Sun & R Siegfried (2003). Instantaneous Spectral Analysis: Detection of Low-Frequency Shadows Associated With Hydrocarbons. The Leading Edge.

Dilay, A., and J. Eastwood, 1995, Spectral Analysis Applied to Seismic Monitoring of Thermal Recovery: The Leading Edge, 14, 1117–1122.

Haris, A and Haryono, 2012, Quantifying Q Factor Derived From Spectral Decomposition for Identifying Hydrocarbon Reservoir: Example From 3D Seismic Real Data: Himpunan Ahli Geofisiska Indonesia,Proceedings PIT HAGI 2012 37th HAGI Annual Convention & Exhibition, Palembang.

Haris, A. and Khair A Suabdi, 2012, Frequency gradient of spectral decomposition for identifying hydrocarbon reservoir – example from indonesian field, Thirty-Sixth Annual Convention & Exhibition, Indonesian Petroleum Association, Jakarta.

Mandong, A., Bekti, R., Saputra, R., 2020. Amplitude Variation with Frequency as Direct Hydrocarbon Indicator for Quick Look and Different Insight of Hydrocarbon Delineation, Jurnal Geofisika (2021) Vol. 19, No. 02 pp. 62-68

Maynard, K., and Morgan, W. A., 2005. Appraisal Of A Complex, Platform Carbonate, Bukit Tua Discovery, Ketapang Psc, East Java Basin, Indonesia: Indonesian Petroleum Association, Proceedings 30th Annual Convention, Jakarta.

Mitchell, J. T., N. Derzhi, and E. Lickman, 1997, Low frequency shadows: The rule, or the exception? 67th Annual International Meeting, SEG, Expanded Abstracts, 685–686.

Sinha, Satish, Partha S. Routh, Phil D. Anno, and John P. Castagna, 2005, Spectral Decomposition of Seismic Data With Continuous-Wavelet Transform, Geophysics, Vol. 70, No. 6, p. 19–25

Wu, X., Li, X., Chapman, M., 2012. Frequency-dependent AVO attribute: Theory and example, First Break 30

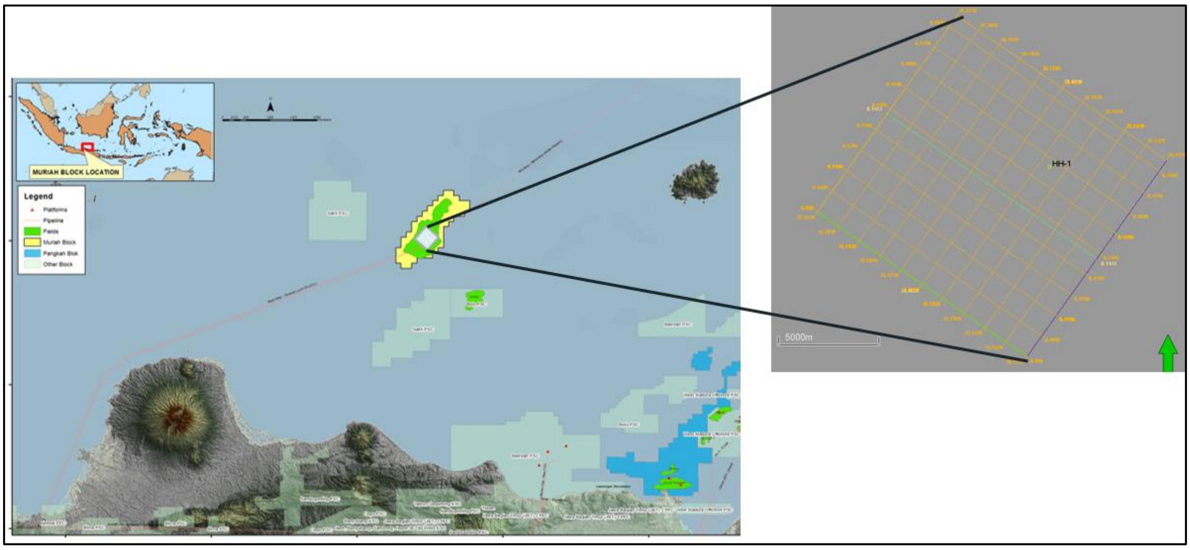

Figure 1 : Location Map and Data Availability

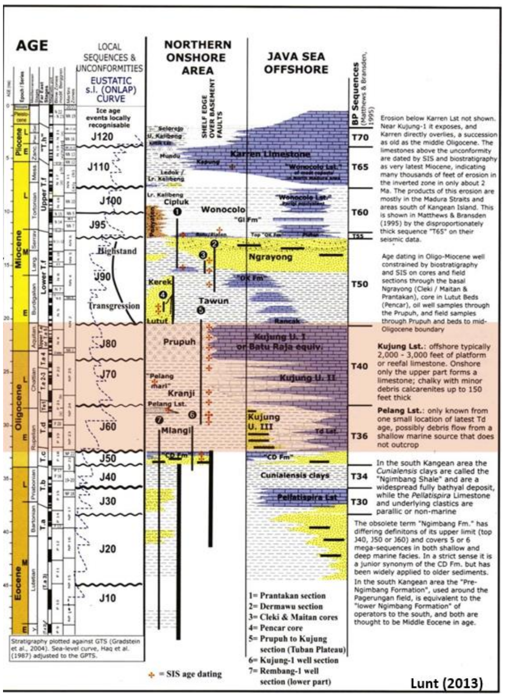

Erosion below Karren Lst not shown. Near Kujung-1 it exposes, and Karren directly overlies, a succession as old as the middle Oligocene. The limestones above the unconformity are dated by SIS and biostratigraphy as very latest Miocene, indicating many thousands of feet of erosion in the inverted zone in only about 2 Ma. The products of this erosion are mostly in the Madura Straits and areas south of Kangean Island. This is shown in Matthews & Bransden (1995) by the disproportionately thick sequence "T65" on their seismic data.

Age dating in Oligo-Miocene well constrained by biostratigraphy and SIS on cores and field sections through the basal Ngrayong (Cleki / Maitan & Prantakan), core in Lutut Beds (Pencar), oil well samples through the Prupuh, and field samples through Prupuh and beds to mid-Oligocene boundary

Kujung Lst.: offshore typically 2,000 - 3,000 feet of platform or reefal limestone. Onshore only the upper part forms a limestone; chalky with minor debris calcarenites up to 150 feet thick

Pelang Lst.: only known from one small location of latest Td age, possibly debris flow from a shallow marine source that does not outcrop

In the south Kangean area the *Cunialensis* clays are called the "Ngimbang Shale" and are a widespread fully bathyal deposit, while the *Pellatispira* Limestone and underlying clastics are parallic or non-marine

The obsolete term "Ngimbang Fm." has differing definitons of its upper limit (top J40, J50 or J60) and covers 5 or 6 mega-sequences in both shallow and deep marine facies. In a strict sense it is a junior synonym of the CD Fm. but has been widely applied to older sediments.

In the south Kangean area the "Pre-Ngimbang Formation", used around the Pagerungan field, is equivalent to the "lower Ngimbang Formation" of operators to the south, and both are thought to be Middle Eocene in age.

Stratigraphy plotted against GTS (Gradstein et al., 2004). Sea-level curve, Haq et al. (1987) adjusted to the GPTS.

✣ = SIS age dating

1= Prantakan section
2= Dermawu section
3= Cleki & Maitan cores
4= Pencar core
5= Prupuh to Kujung section (Tuban Plateau)
6= Kujung-1 well section
7= Rembang-1 well section (lower part)

Lunt (2013)

Figure 2 : Regional Chronostratigraphy

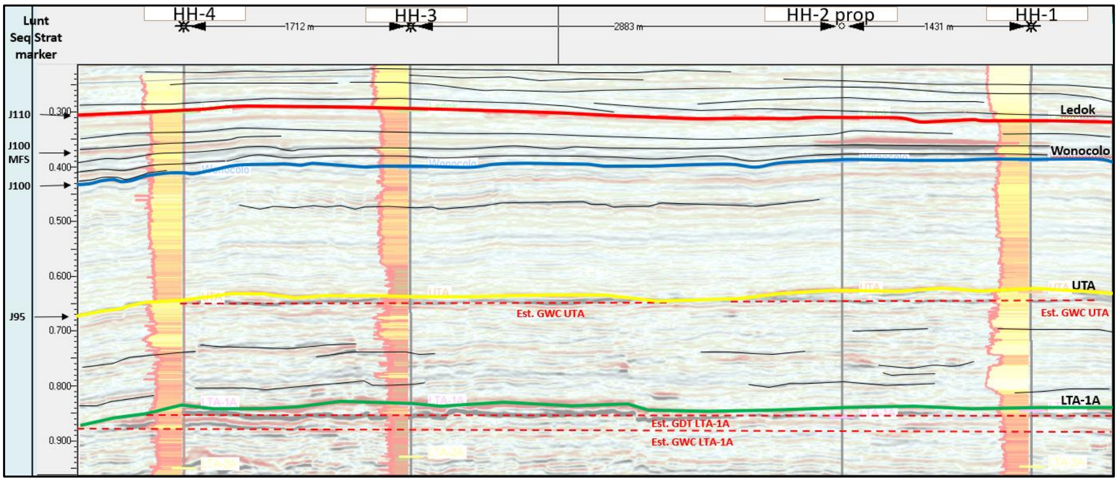

Figure 3 : Well Correlation with seismic background

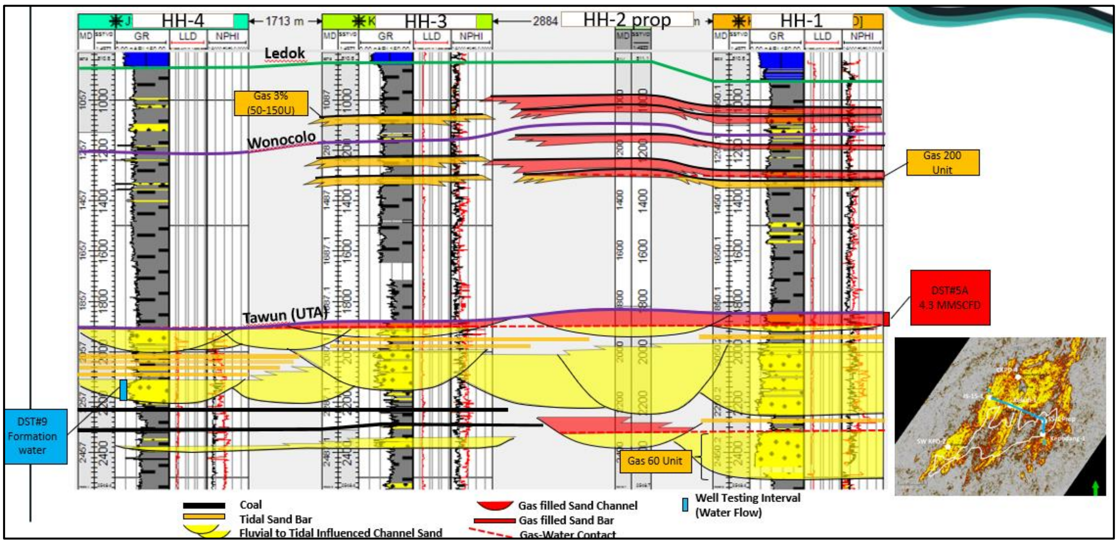

Figure 4 : Well Correlation and facies model

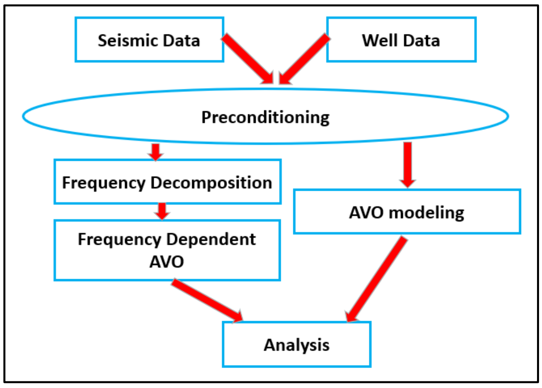

Figure 5 : Workflow

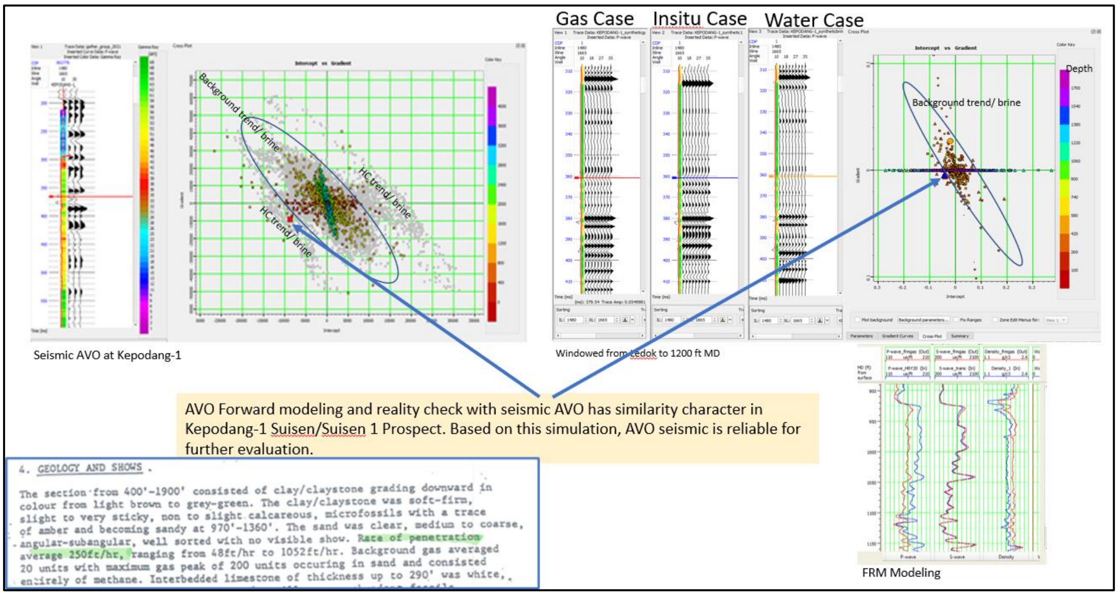

AVO Forward modeling and reality check with seismic AVO has similarity character in Kepodang-1 Suisen/Suisen 1 Prospect. Based on this simulation, AVO seismic is reliable for further evaluation.

4. GEOLOGY AND SHOWS .

The section from 400'-1900' consisted of clay/claystone grading downward in colour from light brown to grey-green. The clay/claystone was soft-firm, slight to very sticky, non to slight calcareous, microfossils with a trace of amber and becoming sandy at 970'-1360'. The sand was clear, medium to coarse, angular-subangular, well sorted with no visible show. Rate of penetration average 250ft/hr, ranging from 48ft/hr to 1052ft/hr. Background gas averaged 20 units with maximum gas peak of 200 units occuring in sand and consisted entirely of methane. Interbedded limestone of thickness up to 290' was white,

Figure 6 : Forward modeling AVO and fluid replacement modeling indicate that reality check with AVO seismic has similarity in HH-1 and shallower prosepct.

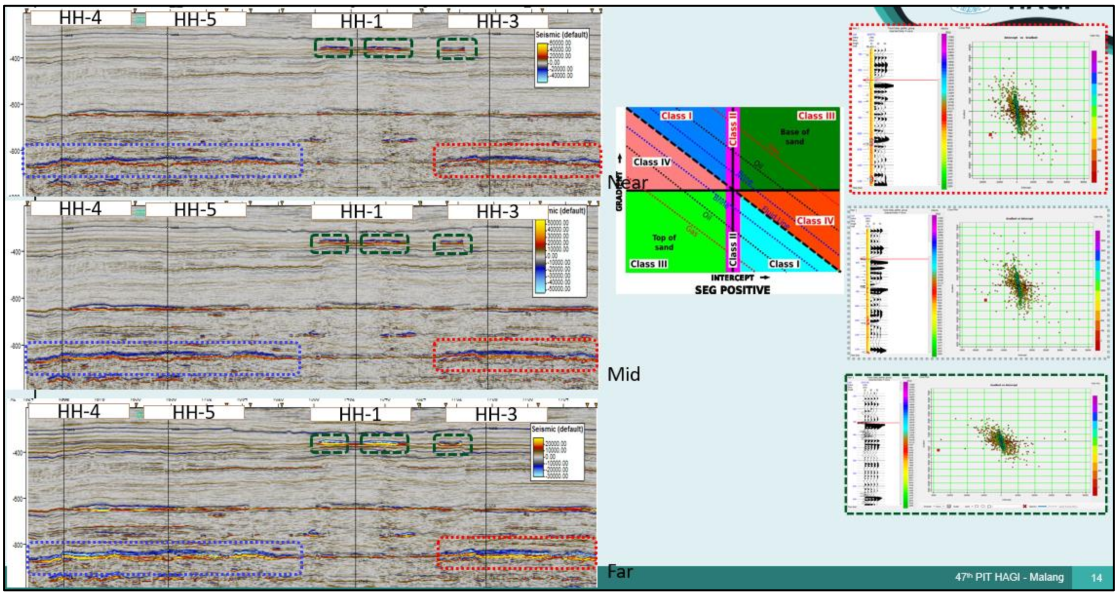

Figure 7 : Amplitude variation offset in several prospects (deeper prospects with proven gas sand red and blue dashed line) and shallower part prospect (green dashed line) which has similar characteristics of AVO respon with deeper prospects.

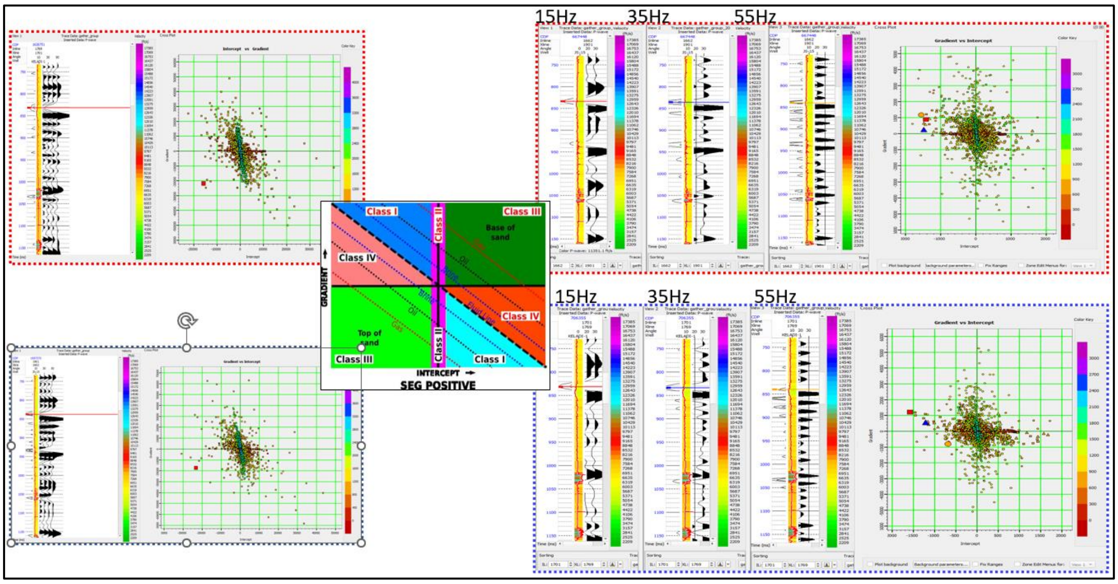

Figure 8 : Conventional AVO and Frequency dependent AVO response and classification in deeper prospect (blue and red dashed line)

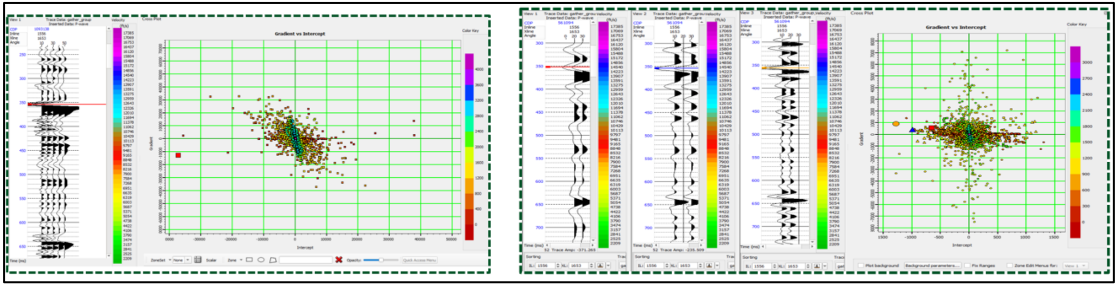

Figure 9 : Conventional AVO and Frequency dependent AVO response and classification in shallower t (green dashed line) which can unlock the new potential play ini this study area.

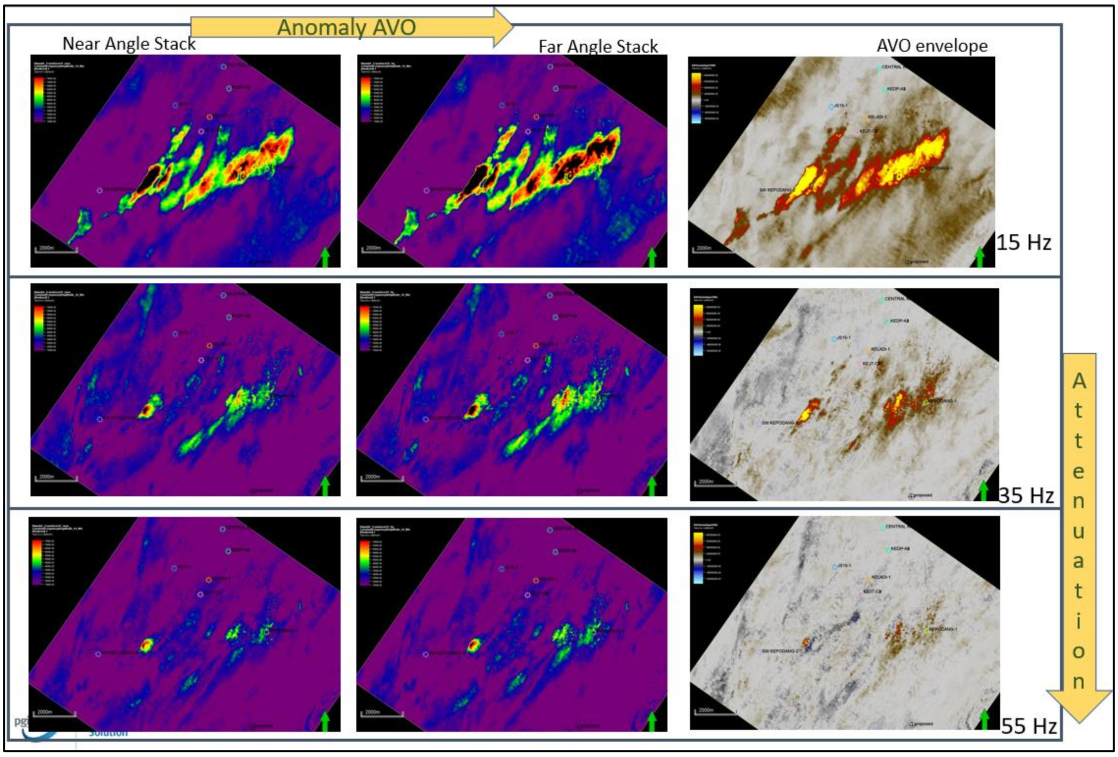

Figure 10 : Conventional AVO and Frequency dependent AVO response lateral distribution which indicate gas sand presence. It will described with increasing anomaly AVO in Far angle stack and attenuation of amplitude in higher frequency.

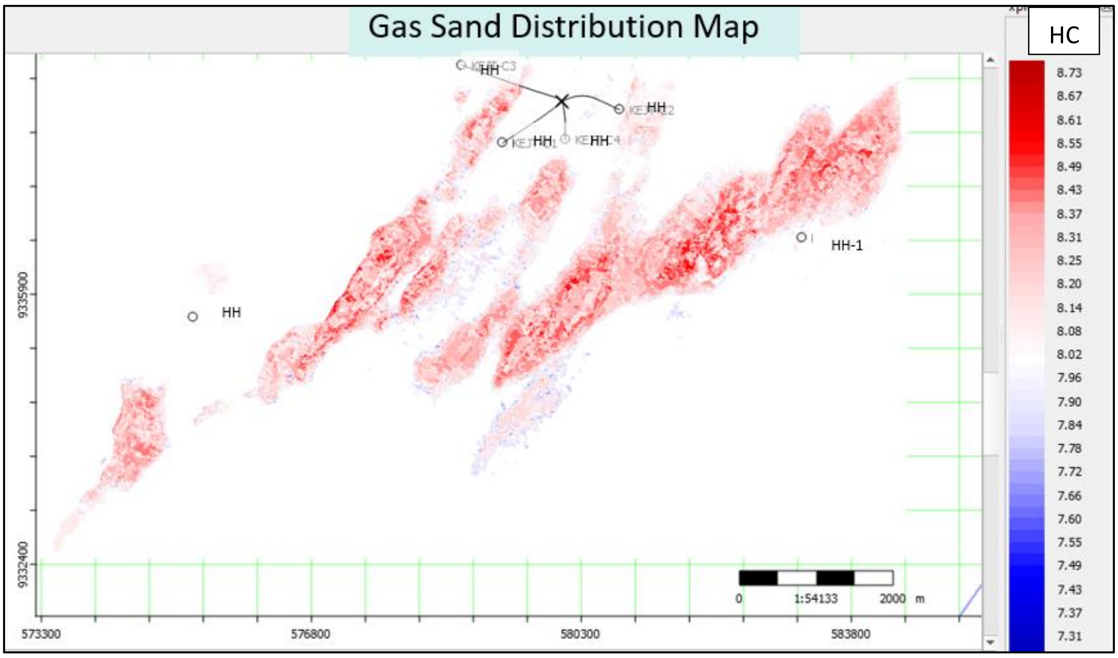

Figure 11 : Lateral distribution of gas sand in shallower prospect which expected to be contributed in existing field.